Journal Pre-proof

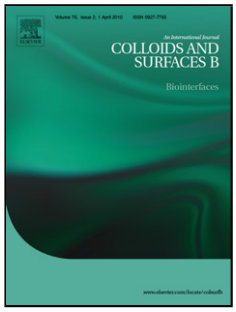

Effects of primary amine-based coatings on microglia internalization of nanogels

Emanuele Mauri, Pietro Veglianese, Simonetta Papa, Arianna Rossetti, Massimiliano De Paola, Alessandro Mariani, Zbyšek Posel, Paola Posocco, Alessandro Sacchetti, Filippo Rossi

PII: S0927-7765(19)30718-0

DOI: https://doi.org/10.1016/j.colsurfb.2019.110574

Reference: COLSUB 110574

To appear in: *Colloids and Surfaces B: Biointerfaces*

Received Date: 5 August 2019

Revised Date: 8 October 2019

Accepted Date: 9 October 2019

Please cite this article as: Mauri E, Veglianese P, Papa S, Rossetti A, De Paola M, Mariani A, Posel Z, Posocco P, Sacchetti A, Rossi F, Effects of primary amine-based coatings on microglia internalization of nanogels, *Colloids and Surfaces B: Biointerfaces* (2019), doi: https://doi.org/10.1016/j.colsurfb.2019.110574

Effects of primary amine-based coatings on microglia internalization of nanogels

Emanuele Mauri[a], Pietro Veglianese[b], Simonetta Papa[b], Arianna Rossetti[a], Massimiliano De Paola[c], Alessandro Mariani[c], Zbyšek Posel[d,e], Paola Posocco[e], Alessandro Sacchetti[a,*] and Filippo Rossi[a,*]

[a] Department of Chemistry, Materials and Chemical Engineering "Giulio Natta", Politecnico di Milano, via Mancinelli 7, 20131 Milan, Italy

[b] Department of Neuroscience, IRCCS Istituto di Ricerche Farmacologiche "Mario Negri", via La Masa 19, 20156 Milan, Italy

[c] Department of Environmental Health Sciences, IRCCS Istituto di Ricerche Farmacologiche "Mario Negri", via La Masa 19, 20156 Milan, Italy

[d] Department of Informatics, Faculty of Science, Jan Evangelista Purkyně University, Ústí nad Labem, Czech Republic

[e] Department of Engineering and Architecture, University of Trieste, via Valerio 17, 34127 Trieste, Italy

[*]Alessandro Sacchetti. Tel.: +39 0223993017; fax: +39 0223993180; e-mail: alessandro.sacchetti@polimi.it

[*]Filippo Rossi. Tel.: +39 0223993145; fax: +39 0223993180; e-mail: filippo.rossi@polimi.it

Graphical abstract

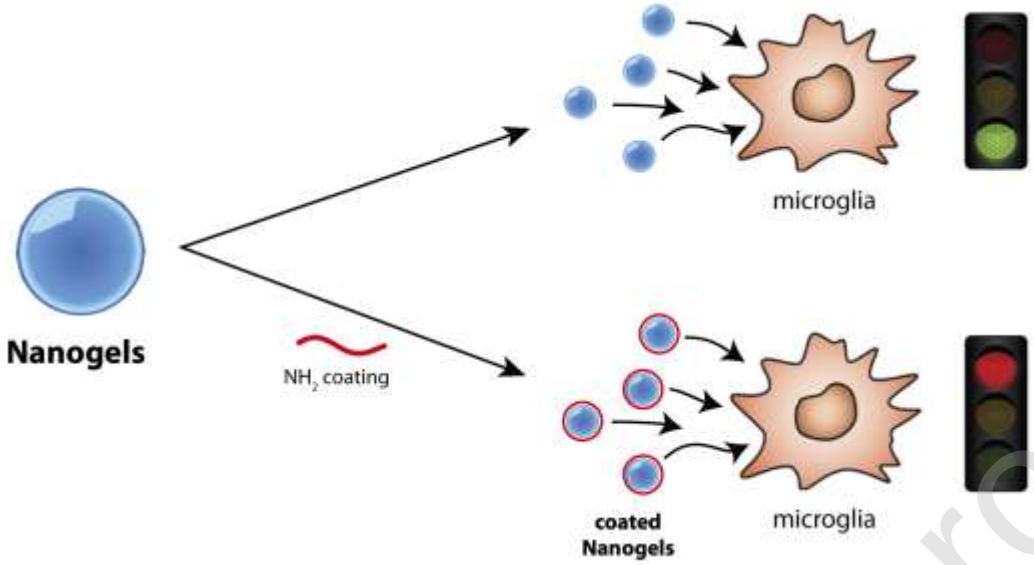

Highlights

- Tuning macrophages uptake allows increasing nanotool availability to other cells
- Primary amine coating of nanogels is not widely investigated as "uptake-control"
- -NH_2 creates interactions with macrophages, affecting the nanogel internalization
- The uptake modulation could be performed using PEGylation combined to -NH_2 groups

Abstract

Nanogels represent a pivotal class of biomaterials in the therapeutic intracellular treatment of many diseases, especially those involving the central nervous system (CNS). Their biocompatibility and synergy with the biological environment encourage their cellular uptake, releasing the curative cargo in the desired area. As a main drawback, microglia are generally able to phagocytize any foreign element overcoming the blood brain barrier (BBB), including these materials, drastically limiting their bioavailability for the target cells. In this work, we investigated the opportunity to tune and therefore

reduce nanogel internalization in microglia cultures, exploiting the orthogonal chemical functionalization with primary amine groups, as a surface coating strategy. Nanogels are designed by following two methods: the direct grafting of aliphatic primary amines and the linkage of -NH_2 modified PEG on the nanogel surface. The latter synthesis was proposed to evaluate the combination of PEGylation with the basic nitrogen atom. The achieved results indicate the possibility of effectively modulating the uptake of nanogels, in particular limiting their internalization using the PEG-NH_2 coating. This outcome could be considered a promising strategy for the development of carriers for drugs or gene delivery that could overcome microglia scavenging.

Keywords: coatings, drug delivery, nanogels, polymer functionalization, microglia.

1. Introduction

Engineered nanosystems have become innovative biomaterials in a wide range of biomedical treatments including drug delivery, tissue engineering, medical diagnosis and monitoring [1-4]. In particular, different strategies have been addressed to cell-targeted therapies, where the aim is the delivery of specific biomolecules, drugs and genes into a desired intracellular area to counteract and minimize the symptoms and the degenerative effects of disorders such as cancer, infections, and neurological and autoimmune deficiencies. Nanoscale systems have shown a promising role in the healing of central nervous system (CNS) inflammations through the selective treatment of microglia, the resident macrophage cells recruited as the first and main form of active immune defense in the CNS and in its inflammatory events. [5, 6]. Due to their role, microglia are able to quickly respond to external stimuli; unfortunately, they can show either a harmful phenotype (M1) or a beneficial one (M2) against the progression of any inflammatory disease [7-9]. In this field, the pivotal aspect is the

ability to provide a biocompatible smart nano-carrier to encapsulate the cargo, promoting its controlled release under specific stimuli and its absorption within the microglia cytosol in a curative way [10-12]. Literature proposes a wide scenario of nanoparticles satisfying these criteria and their efficient uptake in order to tune the cell fate, induce or prevent any phenotype alterations, restore cell-cell communications, and modulate cell structure by phenomena at the nano-bio interface [13, 14]. Among these, nanogels (NGs) play a leading role due to their distinctive features that involve colloidal stability, high specific surface area, high drug encapsulation capacity, minimal toxicity and swelling behavior, thus providing a synergic compliance with the biological environment [15-17]. Moreover, the physico-chemical properties of these nanosystems could be tailored through the rational choice of polymers used and of the possible chemical syntheses, bearing the versatile advantage of the nanogel formulations. In particular, the shape, morphology and elasticity are able to affect targeting, circulation, internalization, immune cell infiltration and adhesion [18, 19].

To date, these devices showed high efficiency in microglia selective treatment [10, 12] but generally in a small portion of the tissue, with consequent promising but partial results. Hence, the possibility to release drugs and biomolecules in a larger portion of the tissue and/or in other cells present in the CNS, such as astrocytes and neurons, remains a big challenge [20]. In this direction, polymer functionalization could be used to introduce specific moieties to overcome these limitations and synthetize nanoscaffolds with distinctive properties: responsive chemical groups, proteins, peptides, polysaccharides and oligonucleotides could be grafted onto the nanogel surface to promote interactions with specific cell receptors, avoiding undesired lysosomal and endosomal trapping, enzymatic degradation or unspecific distribution [21-23]. Studies on amine surface functionalization are proposed to tune cell adhesion on self-assembled monolayers of either cancer or endothelial cells, preserving their viability during the assays [24, 25]. In other works, tertiary and quaternary amino groups were used in the nanogel core to improve gene delivery within the cytosol [26]. For these reasons, in this

work we studied the microglia internalization of nanogels with a different external display of NH_2 moieties. The used NGs are formed by polyethylene glycol (PEG) and linear polyethyleneimine (PEI) and conjugated with a chromophore (rhodamine B) to ensure their *in vitro* detection; the resulting nanoscaffold represents the reference for the cell uptake. The first nanogel functionalization was performed by directly introducing the primary amine moiety on the surface, as a coating layer. The second strategy involves the grafting of PEG modified with primary amine groups (PEG-NH_2), in order to evaluate the effect of a nanogel PEGylation combined with -NH_2. The final comparison between the synthetized reference-nanogels and the amine-coated ones suggests a significant modulation of microglia internalization: the presence of superficial amine groups affects interaction with the transmembrane receptors and the topography of the material, reducing the uptake.

Moreover, the rationale of decorating NGs only with primary amines rather than PEG and -NH_2 moieties gives rise to different coating density and hydration due to the physico-chemical interactions with ions and solvent molecules. Nanogels functionalized with PEG-NH_2 show minimal cell internalization. These results can be considered as a promising perspective to design nanogels as modulating drugs or gene carriers in the CNS.

2. Materials and Methods

2.1 Materials

The experimental procedures required the following polymers for the nanogel design: polyethylene glycol 8000 (M_w = 8 kDa, by Merck KGaA, Darmstadt, Germany) and linear polyethyleneimine 2500 (M_w= 2.5 kDa, by Polysciences Inc., Warrington, USA). All other chemicals were purchased from Merck (Merck KGaA, Darmstadt, Germany) and used as received, without any further purification. Solvents were of analytical-grade purity. All the rhodamine derivatives were stored at 4°C.

2.2 Characterization techniques

Polymer functionalization was evaluated through NMR and FT-IR analyses. ^{1}H-NMR spectra were carried out on a Bruker AC (400 MHz) spectrometer using chloroform ($CDCl_3$) as a solvent, and chemical shifts were reported as δ values in parts per million with respect to tetramethylsilane (TMS) as an internal reference. FT-IR spectra were recorded using the KBr pellet technique for the analyzed samples and a Thermo Nexus 6700 spectrometer coupled to a Thermo Nicolet Continuum microscope equipped with a 15 × Reflachromat Cassegrain objective, at room temperature in air in the wavenumber range 4000–500 cm^{-1}, with 64 accumulated scans and at a resolution of 4 cm^{-1}. The nanogel size, polydispersity index (PDI) and ζ-potential were recorded using the Dynamic Light Scattering (DLS) technique and a Zetasizer Nano ZS from Malvern Instruments. Samples were dissolved in distilled water and the solution was equilibrated for 60 s before data analysis, performed at 37°C. Data shown are an average value of three measurements of each studied nanogel. NG dimensions were also studied with Atomic Force Microscopy (AFM).

Samples were prepared by dropping nanogel latexes onto silicon substrate and then drying. AFM images on 1 × 1 μm areas were then recorded for the preliminary morphologic evaluation; 500 × 500 nm images were then cropped and a height line profile performed for one gel. Surface morphology was evaluated by flattening the images (first order) using NTMDT software.

2.3 Nanogel synthesis

Nanogel synthesis was conducted according to the experimental procedure shown in our previous work [27]. Briefly, PEG hydroxyl groups were modified with imidazole moieties and PEI functionalized with rhodamine B (RhB) using copper-catalyzed azide-alkyne Huisgen cycloaddition (CuAAC) reaction. Two solutions were then prepared separately: in the first, the resulting PEG (200 mg, 0.025 mmol) was dissolved in CH_2Cl_2 (3 mL), while the second was obtained by dissolving PEI conjugated RhB (52 mg, 0.017 mmol) in distilled water (5 mL). The organic solution was added dropwise to the aqueous system under vigorous stirring and the final mixture was sonicated for 30 min. Finally, the polymeric mixture was allowed to stir for 17 h at 25°C (room temperature, r.t.) with the progressive evaporation of CH_2Cl_2 that occurred. The obtained aqueous system was purified through dialysis against slight acid water and lyophilized, resulting in a pink-violet solid. These nanogels were used as a reference for cell internalization, and they were labeled as NG-ref.

2.4 Nanogel coating with -NH_2

The primary amine grafting around the nanogel surface was performed as discussed. NG-ref (15 mg, 0.566 μmol) were dissolved in distilled water (1 mL) and kept under stirring at room temperature.

3-bromopropylamine hydrobromide, the chosen chemical carrying -NH_2 groups (4.95 mg, 22.64 μmol) was dissolved in distilled water (0.5 mL) and added dropwise to the nanogel solution. The mixture was stirred in the dark for 17 h at r.t. Successively, dialysis with regenerated cellulose membrane (M_w cut-off = 6-8 kDa) against distilled water (1000 mL) was performed for 2 days, with daily water exchange, allowing for the removal of unreacted species and potential by-products. The system was frozen at -80°C and the product was finally recovered through lyophilization. Hereinafter, these nanogels coated with primary amine moieties will be indicated as NG-NH_2.

2.5 Synthesis of PEG bis-functionalized azide (PEG-N_3)

PEG functionalization with azide groups was performed by following these two steps: epoxide grafting and ring opening reaction with sodium azide (NaN_3). Chemical modifications involved both terminal hydroxyl groups of the starting PEG.

2.5.1 Epoxide grafting

The first step regarding the reaction of both PEG hydroxyl groups to link epoxide moieties was completed by referring to the Teodorescu procedure [28]: PEG (1 g, 0.125 mmol), excess of epichlorohydrin (293 μL, 3.75 mmol) and NaOH powder (150 mg, 3.75 mmol) were added in sequence in toluene (7 mL), and the reactive system was heated to 50°C for 7 h, maintaining the stirring. The product was recovered by using distilled water (2 x 10 ml) and adding NaCl. The resulting phase was then extracted with CH_2Cl_2 (3 x 15 mL). The resulting organic system was dried over anhydrous sodium sulfate and the solvent removed under reduced pressure.

Diepoxy PEG was obtained as a dry white powder after precipitation in diethyl ether and consequent filtration under vacuum. PEG intermediate was characterized by NMR spectrum. ^{1}H-NMR (400 MHz, CDCl3) δ: 3.57 (s, 720H), 3.12–3.04 (m, 2H), 2.72 (dd, J = 5.1, 4.1 Hz, 2H), 2.54 (dd, J = 5.0, 2.7 Hz, 2H).

2.5.2 Ring-opening reaction and linkage of -N_3 groups

The second step was related to the ring-opening reaction using NaN_3. Diepoxy PEG (500 mg, 0.068 mmol) was dissolved in DMF (10 mL) and then sodium azide (80 mg, 1.23 mmol) and ammonium chloride (131 mg, 2.46 mmol) were added to the solution. The reaction occurred at 60°C in 48 h. The system was concentrated under reduced pressure and the crude was recovered through precipitation in diethyl ether. The solid was re-dissolved in CH_2Cl_2 and the addition of fresh diethyl ether allowed the final precipitation of the desired modified polymer, without by-products. This reaction allowed the linkage of azide moieties and the re-formation of hydroxyl pendant groups. ^{1}H-NMR (400 MHz, CDCl3) δ: 4.10 (m, 2H), 3.58 (s, 720H), 3.28 (d, J = 5.5 Hz, 4H).

2.6 Imidazole activation of PEG-N_3

The previous PEG intermediate (250 mg, 0.03 mmol) was dissolved in acetonitrile (10 mL) and 1,1′-carbonyldiimidazole (CDI, 48.6 mg, 0.3 mmol) was added. The resulting solution was maintained under stirring for 17 h at 45°C. The system was then concentrated under reduced pressure and dialyzed (M_w cut-off = 6-8 kDa) against distilled water for 2 days, by changing the aqueous media every day.

The purified solution was frozen and lyophilized, obtaining PEG with imidazole and azide terminal groups (hereinafter CDI-PEG-N_3). ^{1}H-NMR (400 MHz, CDCl3) δ 7.37 (s, 2H), 7.25 (s, 4H), 4.51–4.45 (m, 4H), 3.60 (s, 720H), 3.29 (d, J = 5.5 Hz, 4H).

2.7 Nanogel coating with CDI-PEG-N_3

CDI-PEG-N_3 (20 mg, 2.4 μmol) was dissolved in 1 mL of DCM, while NGs-ref (15 mg, 0.566 μmol) were dissolved in distilled water (2 mL). The organic phase was added dropwise to the aqueous solution and the mixture was left under stirring for 18 h at r. t.. The resulting solution was dialyzed against distilled water for 1 day, then frozen at -80°C and lyophilized, obtaining nanogel grafting PEG with azide terminal moieties (labeled as NG-N_3)

2.8 Nanogel coating with PEG-NH_2

The final step to obtain the desired primary amine groups on the PEGylated nanogels was proposed as follows [29]. NG-N_3 (10 mg, 0.4 μmol) were dissolved in THF (5 mL) and triphenylphosphine (2 mg, 7.2 μmol) was added and the solution stirred for 4 h at r.t.; distilled water (100 μL) was then added and the reaction system was kept under stirring for another 18 h. Finally, THF, unreacted triphenylphosphine and formed triphenylphosphine oxide were removed *via* dialysis (membrane M_w cut-off= 6-8 kDa) against distilled water for 7 days, with daily water exchange. The produced nanogels with the PEG-NH_2 coating were collected after lyophilization and labeled as NG-PEG-NH_2.

2.9 Primary cell culture

Primary cultures of microglia were obtained from the spinal cord of 13-day-old C57 BL/6J mouse embryos as previously described [30]. Briefly, spinal cords were dissected, exposed to DNAse and trypsin and centrifuged through a BSA cushion. Cells obtained were a population of mixed neuron/glia. These underwent centrifugation through a 6% iodixanol (OptiPrepTM) cushion to separate large neurons from glial cells. The glial fraction was cultured at a density of 25,000 cells/cm^2 into 75 cm^2 flasks, previously pre-coated with poly-L-lysine. Isolated microglia were obtained from flasks containing confluent mixed glial cultures after overnight shaking at 275 rpm in incubators. The supernatants (containing microglia) were collected and seeded at a density of 20,000 cells/cm^2 into 24-well plates. NGs (0.05% weight/volume) were then added to cell cultures for up to 3 days.

2.10 Biocompatibility

After 3 days of culturing, the cytotoxicity of nanogels was evaluated by performing an MTS assay and LDH release. The absorbance was measured at 570 and 490 nm respectively, and the results were compared with those of the control wells to determine relative cell viability.

2.11 Microscope analysis

Fluorescence was acquired at 10× objective magnification (BX61, Olympus, Japan) using a 16 Bit high-resolution camera (Fluoview II, Olympus, Japan) and an appropriate filter cube avoiding cross-talk signals between different fluorochromes. Fluorescent staining was quantified by using the signal segmentation plugin of ImageJ software (http://rsbweb.nih.gov).

2.12 Molecular modeling

A coarse-grained (CG) representation of NG-NH_2 and NG-PEG-NH_2 nanogel surface was used within the dissipative particle dynamics (DPD) framework to provide a molecular view of the surface's behavior [31]. At CG level, a system is represented by DPD segments or beads, which can contain several atoms or molecules depending on the CG level, and can be connected by harmonic springs. Here, we adopted a top-down approach, in which the level of CG is set by mapping the number of water molecules in one water bead. The resulting CG models are reported in Figure S3. An appropriate number of Na^+ and Cl^- ions was added to reproduce the experimental ionic strength. NG surfaces were represented by a collection of PEG/PEI units (bead S) considered as frozen (i.e. not moving) throughout the simulation. To avoid penetration, we also added a reflective layer with bounce-back boundary conditions at the surface-water interface [32].

DPD bead interaction parameters (see Table S1 and Table S2) were calculated using the solubility parameters estimated from the group contribution method by Van Krevelen [33], and mapped into the Flory-Huggins parameter [34]. Electrostatic interactions were taken into account using the approach adopted in [35, 36]. To avoid singularities in the simulations due to the soft-core potential, charges were represented by Gaussian charge clouds [37]. We used the same width of Gaussian distribution for all charged beads together with the standard Ewald summation method with a real-space cutoff equal to zero and a homogenous relative dielectric constant $\varepsilon_r = 80$. Surfaces were represented as a replica of 2D periodic boxes of $L_x = L_y = 9$ nm for the NG-NH_2 system and $L_x = L_y = 15$ nm for the NG-PEG-NH_2 system. Box height L_z was set to 11 and 35 nm, respectively. To match the experimentally low grafting density σ, we set $\sigma = 1.25$ chains/nm^2 for NG-NH_2 and 0.22 chains/nm^2 for NG-PEG-NH_2, which gave us the same number of grafting points in both cases. All simulations were carried out by a LAMMPS [38] package and in-house codes were developed to analyze the trajectories.

NG-NH_2 and NG-PEG-NH_2 systems were generated placing the chains perpendicularly to the NG surface. After an equilibration period, 5000 configurations were stored to calculate water, ions, grafted chain density profiles, grafted chain structural properties (brush height) and the osmotic compressibility. Visualization was performed by VMD software. More details are reported in the SI.

2.13 Statistical analysis

Where applicable, experimental data were analyzed using Analysis of Variance (ANOVA) and a Tukey post-test. Statistical significance was set to p value < 0.05. Results are presented as mean value ± standard deviation.

3. Results and discussion

3.1 Nanogel chemical characterization

Nanogel synthesis was performed by the CH_2Cl_2-in-water emulsification-evaporation method: activated PEG was dissolved in the organic phase, while PEI was dipped in the aqueous solution. After sonication, due to the progressive evaporation of CH_2Cl_2 in the emulsion *status*, the system was able to ensure a homogeneous dispersion of PEG chains around PEI and promote interface interactions between the imidazole and amine moieties, giving rise to the formation of carbamate bonds and the entanglement of the chains. The smart combination of PEG and PEI aims to meet the criteria of biocompatibility with the cellular environment: PEI is a cationic polymer, with a tunable degree of amine protonation according to the pH values [39]. It is characterized by toxic effects on target cells, especially through induction of apoptosis/necrosis when used alone [40, 41]; to overcome this problem, researchers have proposed the grafting of PEG as a non-ionic and non-immunogenic hydrophilic polymer, able to promote high solubility in water, and improved biocompatibility for the final nanogel system [42]. Here, imidazole PEG functionalization was conducted in excess of CDI to ensure the complete conversion of the hydroxyl terminal groups of PEG. On the other hand, PEI functionalization with RhB was addressed by only modifying a reduced percentage of amine groups, preserving most of them for the reaction with CDI-PEG, as we have widely discussed in our previous work [27] on nanostructure design. The carbamate linkage (Figure 1) could be recognized in the ^{1}H-NMR spectrum at 4.28 ppm (methylene proton signals of the PEG terminal monomers involved in the reaction) and at 3.48 ppm (corresponding to the -CH_2 moieties of the PEI monomer forming the nanogel bond). FT-IR analysis showed the carbamate bond at 3400 cm^{-1} (N-H stretch, **1**), 1740 cm^{-1} (C=O stretch, **2**), 1215 cm^{-1} (C-O symmetric) and 1038 cm^{-1} (C-O asymmetric) as reported in Figure 1.

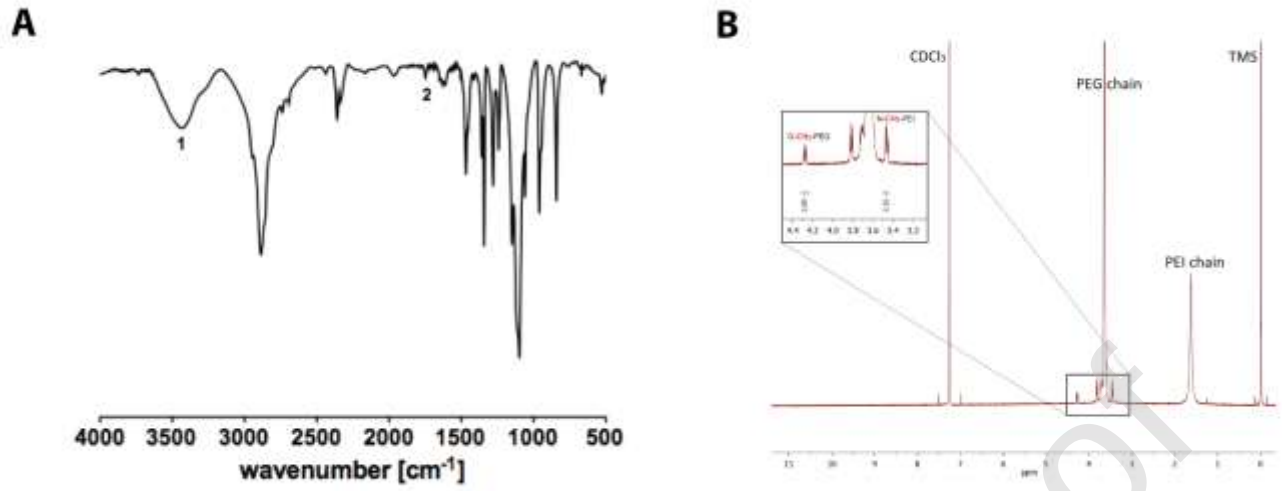

Figure 1. A) FT-IR characterization of PEG-PEI NGs; B) ^{1}H-NMR of PEG-PEI NGs (in red) compared to the spectra of starting modified polymers: imidazole functionalized PEG (in blue) and RhB modified PEI (in black). The chemical shifts of methylene protons of PEG (°) and PEI (*) involved in NG formation are marked.

3.2 Nanogel coating strategies

The effect of amine groups covering the nanogel surface was investigated using 3-bromopropylamine and PEG modified terminal -NH_2. The first was representative of a -CH_2-*spacer* with terminal -NH_2, whereas the choice of the second one was addressed to investigate the combination of a PEGylation with the effect of -NH_2 moieties. 3-bromopropylamine nucleophilic substitution occurred on the residual PEI amine groups and this reaction did not affect the nanogel bonds, preserving the polymeric chains' structural organization. Otherwise, the CDI-PEG-N_3 (characteristic FT-IR signal in Figure 3, wavenumber 2100 cm^{-1}) grafting was performed in CH_2Cl_2-in-water emulsion, giving rise to a progressive formation of the carbamate bonds among the polymeric coating and the PEI secondary amines. No competition was observed between this reaction and the nanogel structural bonds, as demonstrated by the preservation of the latter corresponding signals in NMR and FT-IR analyses, after coating. A reaction scheme regarding NG-ref, NG-NH_2 and NG-PEG-NH_2 is reported in Figure 2.

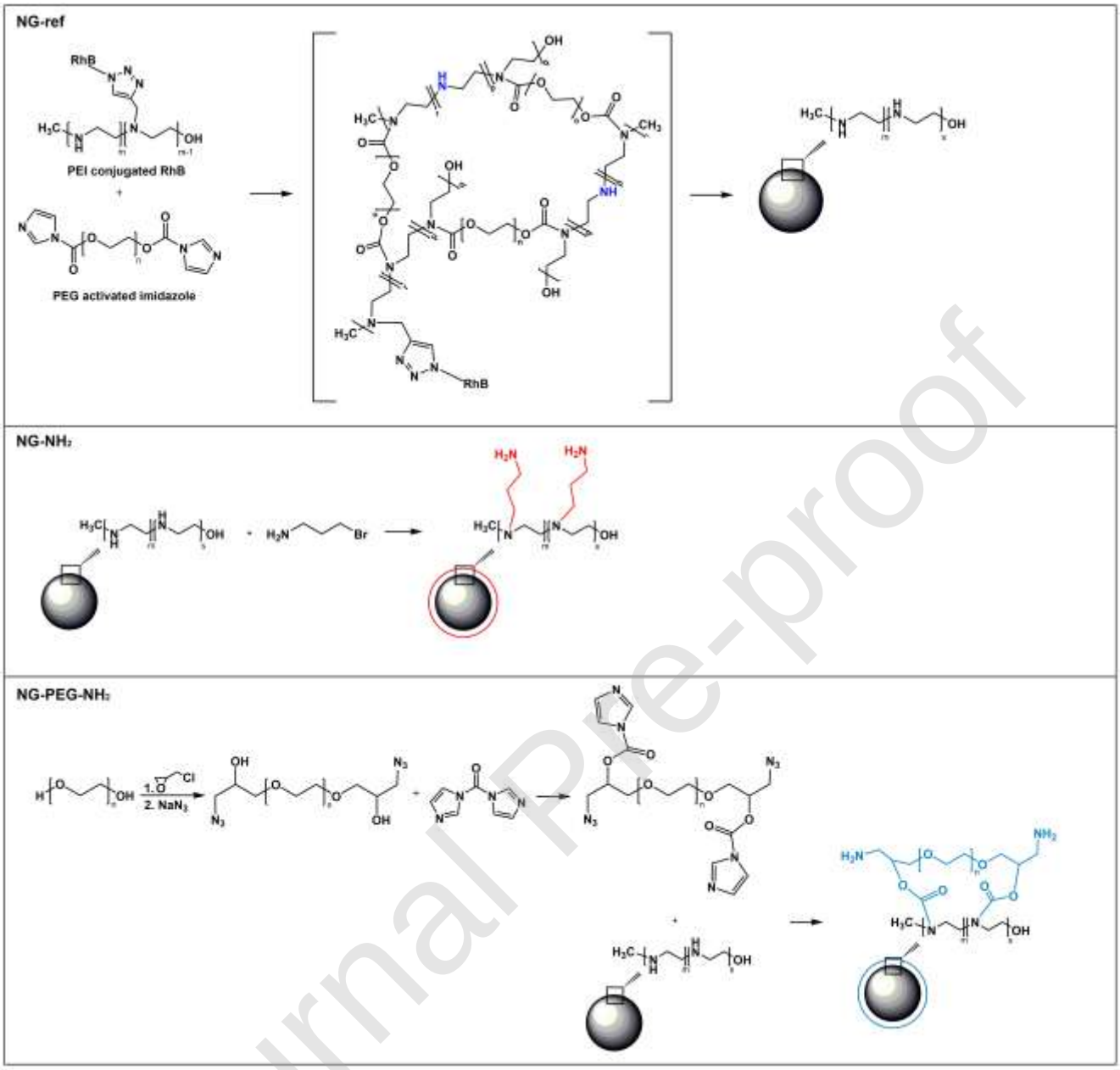

Figure 2. Scheme of nanogel synthesis and resulting putative structures of NG-ref, NG-NH_2 and NG-PEG-NH_2. PEI residual amine groups are highlighted in blue, while the structure of the coating is in red and light blue.

In particular, the amine decoration in NG-NH_2 was performed in a single operation through the reagent's addition to the nanogel solution, whereas the grafting of PEG-NH_2 required two target points: the presence of PEG terminal hydroxyl groups activated with imidazole and the introduction of NH_2 moieties. These were carried out through epoxide functionalization and the consequent ring-opening reaction able to restore the PEG terminal -OH group and introduce the azide in one pot. The former was easily activated by CDI, whereas the latter allowed the correct nanogel coating, providing the necessary nitrogen reactive sites after being converted to primary amines through the triphenylphosphine reaction. FT-IR spectra (Figure 3) show the distinctive peaks of PEG functionalization steps. The characteristic signals of PEG chains are detectable in the wavenumber range 1470 ÷ 800 cm^{-1}. Moreover, a chemical comparison between the three investigated nanogel samples NG-ref and the two NG-NH_2 is illustrated in the Electronic Supplementary Information. In terms of FT-IR spectra, NG-NH_2 and NG-PEG-NH_2 showed the same peaks and therefore, for the sake of clarity, only NG-NH_2 is presented in SI. Together with the above-mentioned PEG signals, PEI exhibits characteristic imide group absorptions around 1790-1725 cm^{-1} (carbonyl stretching), and C-N stretching and bending at 1355 and 745 cm^{-1}.

3.3 Nanogel physical characterization

Potential coating effects on nanogel physical features were investigated using the DLS technique: the hydrodynamic diameter could be affected by either the solvation effect or the protonation of amine groups in water, whereas the PEGylation could improve the hydrophilicity of the nanonetwork and modify the swelling behavior. The recorded data on size and ζ-potential of the three nanogel samples are reported in Table 1.

Table 1. Nanogel DLS (mean values, n = 3) and AFM measurements in PBS.

	DLS			**AFM**
Nanogel	**Diameter (nm)**	**PDI (-)**	**ζ-potential (mV)**	**Diameter (nm)**
NG-ref	190	0.15	0.01	200
NG-NH_2	155	0.20	3.1	180
NG-PEG-NH_2	260	0.18	4.6	285

All samples were characterized by diameter values enabling potential active or passive cellular internalization [43]: in detail, NG-PEG-NH_2 were larger than NG-ref and their interactions with living cells, including the uptake efficiency, the internalization pathway and the intracellular localization could be strongly influenced by their dimensions. The difference in size was mainly related to the grafting of further PEG chains around the nanonetwork which, in addition to the increased steric hindrance, improved the hydrophilicity nature and the swelling of the nanogels themselves. In detail, depending mostly on the polymer-solvent interactions, a higher interaction (due to the PEG hydrophilicity) leads to a higher swelling, with a resulting bigger nanogel diameter [44, 45]. The distributed positive charge on the NG-PEG-NH_2 sample (an increase of 37.8 mV compared to NG-ref ζ-potential in water and 4.6 mV in PBS) was related to the presence of -NH_2 surface groups that gave rise to a nanogel protonation and a positive charged interface. The positive ζ-potential in NG-NH_2 was related to the same protonation mechanism occurring in NG-PEG-NH_2. The coating's different spatial rearrangement is responsible for the smaller dimension of NG-NH_2 with respect to NG-ref. All samples presented a neutral or only slightly positive charge in PBS due to the contribution of the PEI component in nanogel synthesis: the secondary amine groups between the carbon aliphatic CH_2-CH_2 spacer were subjected to protonation behavior [46, 47].

The evolution of the particle size and PDI versus time is reported in Figure 3A and 3B, respectively. From Figure 3, it is possible to observe that the NG-ref remain substantially unaltered; in fact, only minor changes are observed, which can be attributed to the spatial rearrangement. It is also worth noting that this also happens for coated NGs, finally proving the efficiency of the added coating strategies.

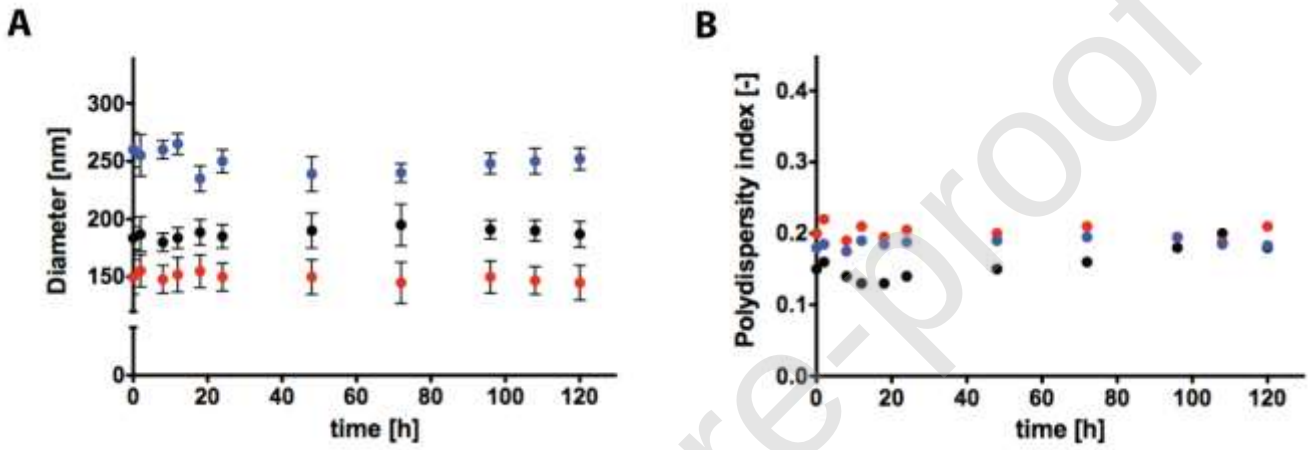

Figure 3. Particle size (n = 3) (A) and PDI (B) versus time of NG-ref (black circles), NG-NH_2 (red circles) and NG-PEG-NH_2 (blue circles).

NG dimensions and morphologies were also analyzed by AFM analysis (Figure 4): all particles showed a spherical and smooth surface. NG sizes are comparable to those recorded in DLS with only slight variations. These variances are due to the different sample processing between DLS and AFM: the first analysis is performed in aqueous solutions (measures hydrodynamic radius) where swelling contribution is present, whereas in the second, the measurement is conducted in dry state.

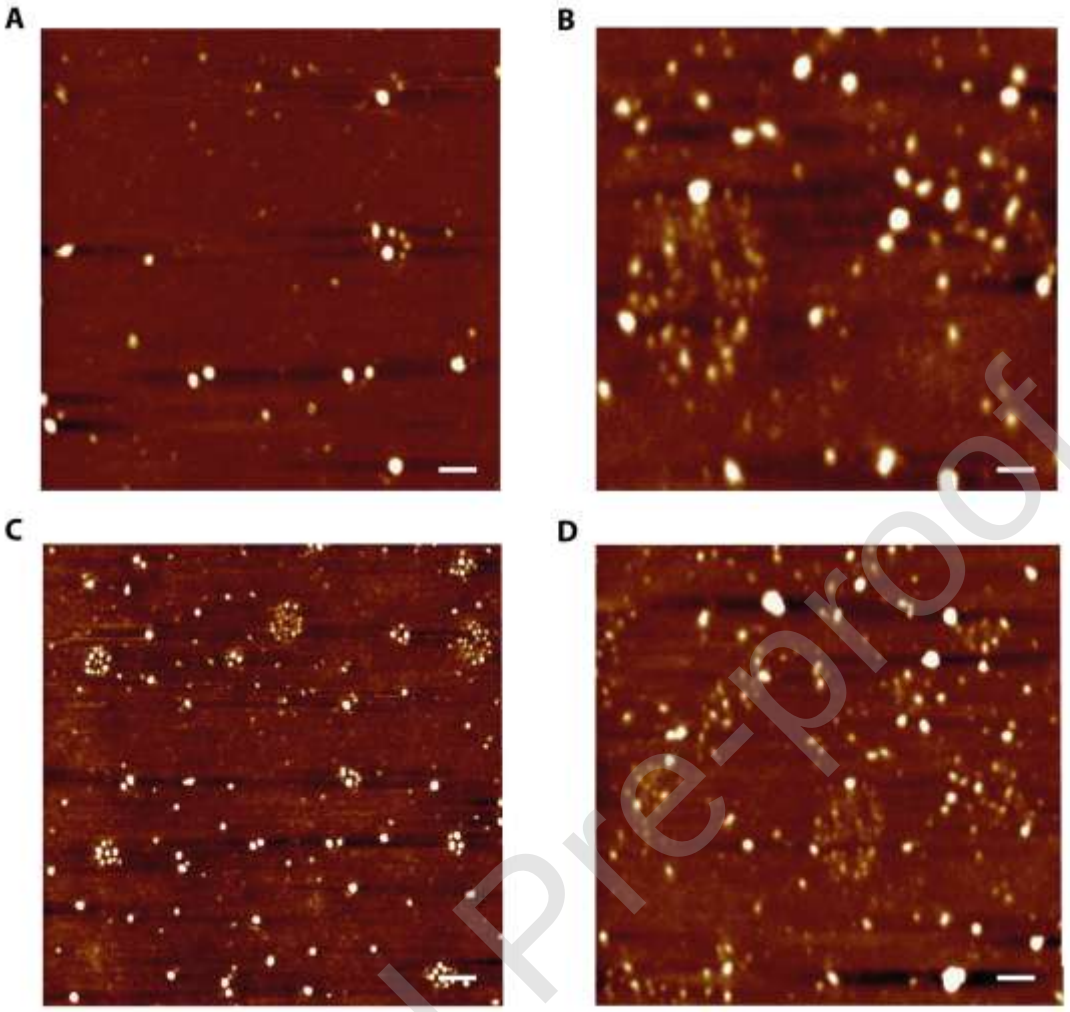

Figure 4. AFM images of fluorescent coated nanogels: (A, C) NG-NH_2 and (B, D) NG-PEG-NH_2. Scale bars: 500 nm (A, B), 1000 nm (C, D).

3.4 Molecular modeling of the nanogel surface

In the last years many computational techniques demonstrated to be accurate in the study of coatings and surface package density. In this direction the most accurate computational approaches to model polymer brushes are the so-called atomistic simulations, in which every atom and bond of the system is represented in an explicit way and all occurring interactions are accounted for.

Unfortunately, at this level of precision slow-equilibrating phenomena such as the relaxation of high molecular weight chains is computationally unfeasible. As a consequence, the best compromise is to reduce some degrees of freedom for the system by averaging a molecule into a number of coarse-grained particles. This simplified representation of the structure, and of the underlying interactions, allows for longer length and time scales than atomistic models. Many different techniques were developed in this field, and they all go under the common name of "coarse-grained (CG)" models. Here, we employed a CG method called Dissipative Particle Dynamics (DPD), which was already successfully used for predicting the scaling and phase behavior of polymer brushes [48] and the solvent-responsive brushes in smart nanofluidic devices [49, 50]. A molecular view of NG-NH_2 and NG-PEG-NH_2 surface features obtained with CG method is visible in Figure 5 (left panels). Simulations clearly show that the NG-PEG-NH_2 surface is much more shielded than that of the NG-NH_2 by polymer chains extending deeply into the solvent. Averaged density profiles provide an overall picture of the distribution of water, ions, and coating chains close to the NG surface for both functionalizations (Figure 5, right panels).

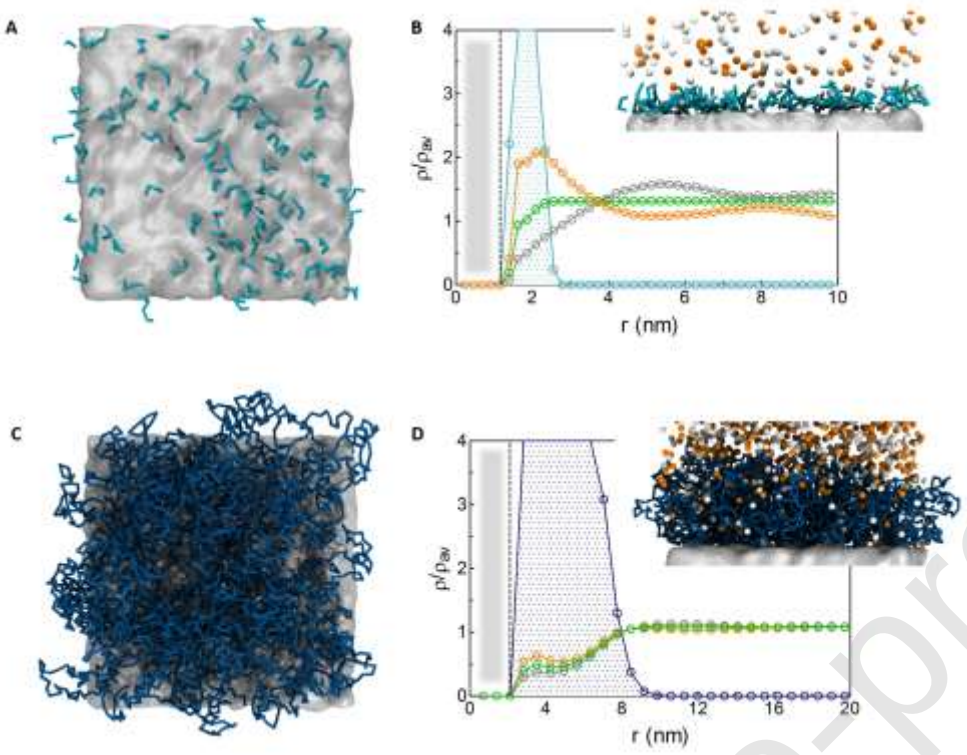

Figure 5. Top-view snapshots obtained by DPD calculation of NG-ref surface (grey shaded area) grafted by primary amines (NG-NH_2) (**A**) or PEG modified with primary amine groups (NG-PEG-NH_2) (**C**). Water, ions, and monomer averaged density profiles for NG-NH_2 (**B**) and NG-PEG-NH_2 (**D**) as a function of the distance from the NG-ref surface (shaded in grey). Panels in B and D show a front-view configuration for each system. Sodium and chlorine ions are depicted as white and orange spheres, respectively. For reasons of clarity, water is not shown. Densities in B and D are scaled by the average density of each species. Density color legend: water - green; chlorine - orange; sodium - grey; NG-NH_2 - light blue; NG-PEG-NH_2 - blue. Dotted lines highlight the NG-ref surface.

For the NG-PEG-NH_2 nanoparticles, the polymer layer extends approximately 8 nm out from the NG-ref surface and, on average, water molecules and ions diffuse deeply into the coating, thus mediating interactions with the external environment.

Due to their short length and low grafting density, NG-NH_2 chains stay close to the surface, which is almost well-exposed to the solution. Layering of negative charges is also visible in correspondence of the NG-NH_2 surface as a result of the counterbalance of the positively charged terminal amines.

Spatial distribution of the density of each system component (i.e. monomers, water molecules and ions) may be very informative on lateral structural inhomogeneity of a surface. This aspect is crucial, since local molecular properties are known to direct the behavior of nanomaterials at bio-interfaces (and vice-versa) and are not always easily accessible by experiments. Two-dimensional density profiles were thus calculated at the average height of each external shell (the so called "brush height*"* [49]), since they describe the first interface the NG exposes to the solvent and external environment (e.g. cells) (Figure 6). The comparison of Figure 6A and E highlights that NG-NH_2 and NG-PEG-NH_2 have a different hydration level; while for NG-PEG-NH_2 water distribution is rather homogenous and close to the hydration level of the unmodified NG-ref surface, for NG-NH_2 solvent molecules are not uniformly distributed with local values that are 1.4 times those present in the unmodified NG-ref. The same also holds for Na^+ and Cl^- ions, as well as for polymer moieties. In NG-NH_2 the short, dangling and charge-ended chains generate local inhomogeneities which shape the overall NG topography; in NG-PEG-NH_2 the charged amines are localized close to the surface and screened by the thick PEG layer that mediates interactions with the exterior, and leads to an interface fairly similar to NG-ref in terms of water and ion distribution. Moreover, compressibility studies underlined that NG-NH_2 are three times more rigid than NG-PEG-NH_2.

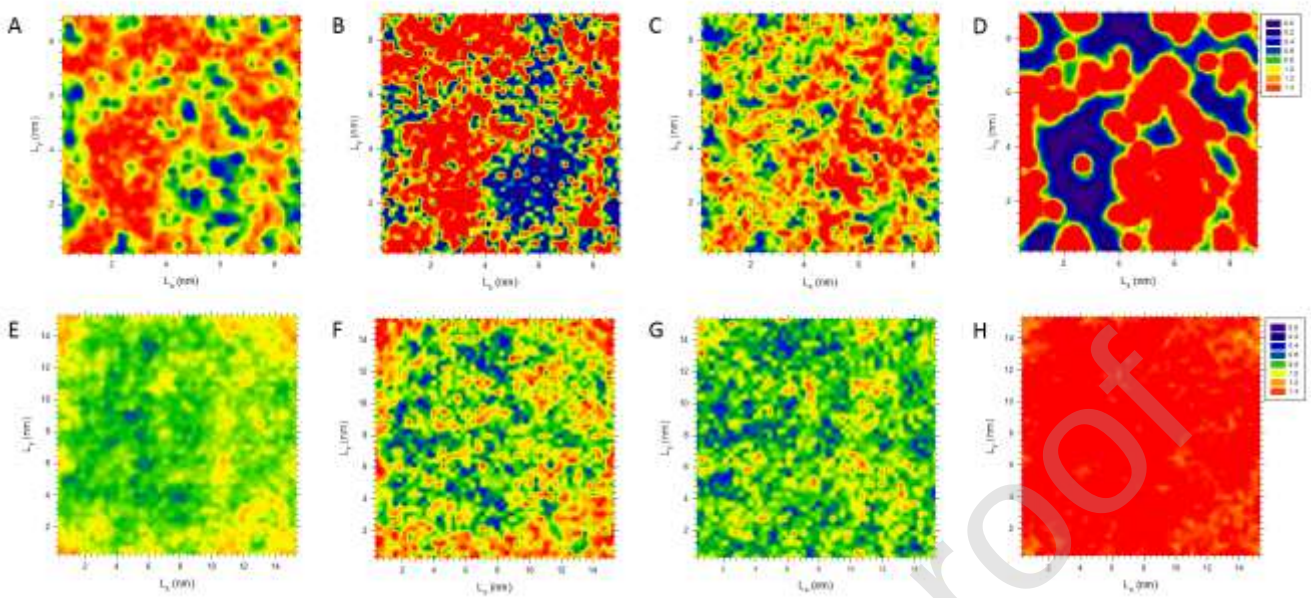

Figure 6. Two-dimensional density maps of water (**A** and **E**), Na^+ (**B** and **F**) Cl^- (**C** and **G**), and chains (**D** and **H**) at the brush height for NG-NH_2 (**A**-**D**) and NG-PEG-NH_2 (**E**-**F**). Water and ion density (i.e. the number of molecules per unit area) is scaled to the corresponding value in the NG-ref. The number of polymer monomers per unit area is normalized to the average polymer value.

3.5 In vitro biocompatibility and microglia uptake

The synthetized NGs were first evaluated as biocompatible nanoscaffolds in a biological environment. *In vitro* cytotoxicity tests were evaluated by culturing microglia for 3 days, while sharing the medium with the nanogels and then measured with MTS assay (Figure 7A). The nanogel amount dissolved in the cell medium is in accordance with the concentration range used in pharmacological treatments and in biomedical applications. The protocol is commonly used as a biocompatibility test for colloidal suspensions. Figure 7A shows cell viability in the presence of NG-ref, NG-NH_2 and NG-PEG-NH_2: the similar cell trend in all samples, and compared to the cells without nanogel treatment (CTRL), is clearly visible.

No decrease in viability was recorded, indicating that the nanonetwork was compatible and chemical functionalization did not induce toxic or side-effects. The influence of surface functionality on nanogel uptake and clearance by microglia is shown in Figure 7B, considering cell exposure to the nanonetworks for 24 h. Red signals are representative of nanogel structures traceable due to the rhodamine moiety [30]: as indicated in Figure 7C, NG-ref were characterized by significant cellular internalization, whereas NG-NH_2 samples were less phagocytized (approximately half of the NG-ref amount) and the smart combination of PEGylation and amine groups allowed for minimal microglia uptake. All data were characterized by a significant statistical difference ($p < 0.001$), suggesting that the chemical grafting of different groups could be a promising approach to direct the tuning of the nanogel pathway in a cellular medium. In particular, the presence of amine groups (NG-NH_2) as a superficial contact with cell surface receptors seemed to provide reduced nanogel intracellular distribution. Indeed, the NG-ref and NG-NH_2 samples share comparable hydrodynamic diameters, differing primarily in their surface chemistry. Coupled with the theoretical calculations, this seems to support the hypothesis that functionalization with amines endows NGs with specific surface properties (inhomogeneous topography, high hydration) and a protonation state that could have decreased adhesion to cells and activated a different microglia response. The introduction of PEG-NH_2 functionalization allowed for combining the chemical amine effect to the polymer hydrophilicity, resulting in a spatial rearrangement of the polymeric structure and the increase of the nanogel dimension. Another possible explanation is represented by the different mechanical properties related to the introduced coatings. It is indeed well known that they can influence and regulate cell behavior once they come into contact [51].

This electrostatic-physical conjunction designed a nanotool that satisfies the criteria of potential cellular internalization but, due to its functionalization, was able to minimize the immune phagocytic uptake, preserving its bioavailability for other cell populations. Therefore, the microglia response could be modulated through the application of smart orthogonal chemical strategies at the nanoscale level.

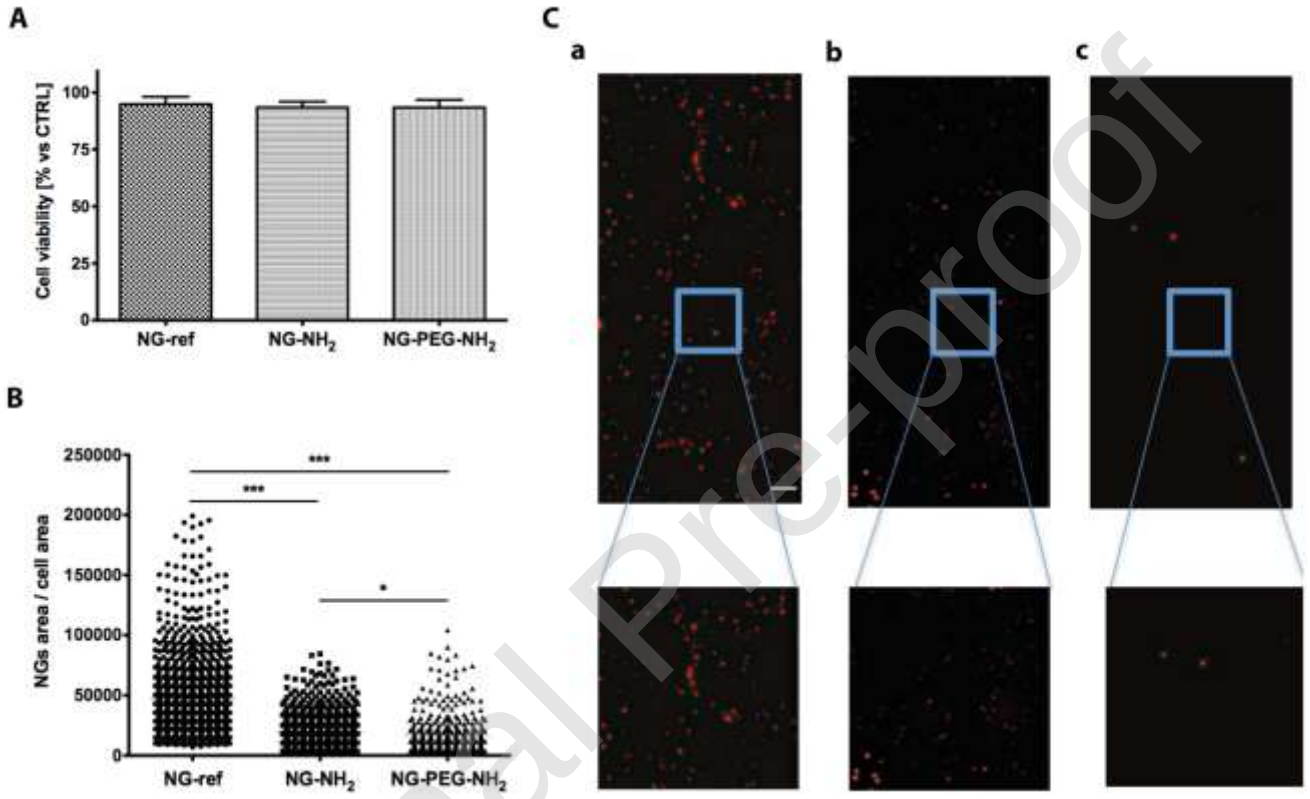

Figure 7. (A) Microglia viability after incubation for 3 days in the presence of nanogels. The columns represent the mean ± S.D.; n = 3. (B) Uptake quantification of nanogels with different coatings after three days of exposure (n = 3). (C) Microglia uptake *in vitro* of NG-ref (a), NG-PEG-NH_2 (b) and NG-NH_2 (c) after 24 h. These images were acquired in dark field at 20 × objective magnification by fixing the same level of color intensity. Red spots represent NGs. Only the culture of microglia treated with NG-ref system shows evident traces of internalization (high density of red spots). This result confirms the efficacy of coating layers with amino derivatives in inhibiting the internalization of nanogels from microglia (scale bar = 500 nm).

4. Conclusions

In this work, we proposed different nanogel coating approaches based on the grafting of primary amines as superficial interacting groups with microglia culture. In particular, the pure grafting of -NH_2 moieties allowed for the reduction of nanogel internalization and minimal uptake was performed by combining amines to nanogel PEGylation. NG-PEG-NH_2 samples satisfied all biocompatible criteria and even if their dimensions were suitable for microglia phagocytic activity, they remained available in high amounts in the extracellular environment. This condition suggested the possible use of these nanonetworks as drug or gene delivery systems for the selective treatment of cells that are different to microglia in central nervous system diseases.

Disclosure

The authors have no relevant affiliations or financial involvement with any organization or entity with a financial interest in or financial conflict with the subject matter or materials discussed in the manuscript.

References

[1] Subbiah R, Veerapandian M, Yun KS. Nanoparticles: Functionalization and Multifunctional Applications in Biomedical Sciences. Curr Med Chem 2010;17:4559-77.

[2] McNamara K, Tofail SAM. Nanoparticles in biomedical applications. Adv Phys-X 2017;2:54-88.

[3] Chinen AB, Guan CM, Ferrer JR, Barnaby SN, Merkel TJ, Mirkin CA. Nanoparticle Probes for the Detection of Cancer Biomarkers, Cells, and Tissues by Fluorescence. Chem Rev 2015;115:10530-74.

[4] Perale G, Veglianese P, Rossi F, Peviani M, Santoro M, Llupi D, et al. In situ agar–carbomer hydrogel polycondensation: A chemical approach to regenerative medicine. Mater Lett 2011;65:1688-92.

[5] Sierra A, Abiega O, Shahraz A, Neumann H. Janus-faced microglia: Beneficial and detrimental consequences of microglial phagocytosis. Frontiers in Cellular Neuroscience 2013;7:6.

[6] Loane DJ, Byrnes KR. Role of Microglia in Neurotrauma. Neurotherapeutics 2010;7:366-77.

[7] Rangarajan P, Karthikeyan A, Dheen ST. Role of dietary phenols in mitigating microglia-mediated neuroinflammation. NeuroMolecular Medicine 2016;18:453-64.

[8] Kapoor K, Bhandare AM, Farnham MMJ, Pilowsky PM. Alerted microglia and the sympathetic nervous system: A novel form of microglia in the development of hypertension. Respiratory Physiology & Neurobiology 2016;226:51-62.

[9] Su F, Yi H, Xu L, Zhang Z. Fluoxetine and S-citalopram inhibit M1 activation and promote M2 activation of microglia in vitro. Neuroscience 2015;294:60-8.

[10] Papa S, Caron I, Erba E, Panini N, De Paola M, Mariani A, et al. Early modulation of pro-inflammatory microglia by minocycline loaded nanoparticles confers long lasting protection after spinal cord injury. Biomaterials 2016;75:13-24.

[11] Papa S, Ferrari R, De Paola M, Rossi F, Mariani A, Caron I, et al. Polymeric nanoparticle system to target activated microglia/macrophages in spinal cord injury. J Control Release 2014;174:15-26.

[12] Cerqueira SR, Oliveira JM, Silva NA, Leite-Almeida H, Ribeiro-Samy S, Almeida A, et al. Microglia response and in vivo therapeutic potential of methylprednisolone-loaded dendrimer nanoparticles in spinal cord injury. Small 2013;9:738-49.

[13] Behzadi S, Serpooshan V, Tao W, Hamaly MA, Alkawareek MY, Dreaden EC, et al. Cellular uptake of nanoparticles: journey inside the cell. Chem Soc Rev 2017;46:4218-44.

[14] Panday R, Poudel AJ, Li X, Adhikari M, Ullah MW, Yang G. Amphiphilic core-shell nanoparticles: Synthesis, biophysical properties, and applications. Colloids and Surfaces B: Biointerfaces 2018;172:68-81.

[15] Mauri E, Perale G, Rossi F. Nanogel Functionalization: A Versatile Approach To Meet the Challenges of Drug and Gene Delivery. ACS Applied Nano Materials 2018;1:6525-41.

[16] Zhang H, Zhai YJ, Wang J, Zhai GX. New progress and prospects: The application of nanogel in drug delivery. Mat Sci Eng C-Mater 2016;60:560-8.

[17] Neamtu I, Rusu AG, Diaconu A, Nita LE, Chiriac AP. Basic concepts and recent advances in nanogels as carriers for medical applications. Drug Deliv 2017;24:539-57.

[18] Anselmo AC, Zhang MW, Kumar S, Vogus DR, Menegatti S, Helgeson ME, et al. Elasticity of Nanopartides Influences Their Blood Circulation, Phagocytosis, Endocytosis, and Targeting. Acs Nano 2015;9:3169-77.

[19] Rossi F, Ferrari R, Castiglione F, Mele A, Perale G, Moscatelli D. Polymer hydrogel functionalized with biodegradable nanoparticles as composite system for controlled drug delivery. Nanotechnology 2015;26:015602.

[20] Dong X. Current strategies for brain drug delivery. Theranostics 2018;8:1481-93.

[21] Blanco E, Shen H, Ferrari M. Principles of nanoparticle design for overcoming biological barriers to drug delivery. Nat Biotechnol 2015;33:941-51.

[22] Soni KS, Desale SS, Bronich TK. Nanogels: An overview of properties, biomedical applications and obstacles to clinical translation. J Control Release 2016;240:109-26.

[23] Silva CSO, Lansalot M, Garcia JQ, Taipa MT, Martinho JMG. Synthesis and characterization of biomimetic nanogels for immunorecognition. Colloids and Surfaces B: Biointerfaces 2013;112:264-71.

[24] Lee JH, Jung HW, Kang IK, Lee HB. Cell Behavior on Polymer Surfaces with Different Functional-Groups. Biomaterials 1994;15:705-11.

[25] Arima Y, Iwata H. Effects of surface functional groups on protein adsorption and subsequent cell adhesion using self-assembled monolayers. J Mater Chem 2007;17:4079-87.

[26] Tamura A, Oishi M, Nagasaki Y. Efficient siRNA delivery based on PEGylated and partially quaternized polyamine nanogels: Enhanced gene silencing activity by the cooperative effect of tertiary and quaternary amino groups in the core. J Control Release 2010;146:378-87.

[27] Mauri E, Moroni I, Magagnin L, Masi M, Sacchetti A, Rossi F. Comparison between two different click strategies to synthesize fluorescent nanogels for therapeutic applications. Reactive and Functional Polymers 2016;105:35-44.

[28] Teodorescu M, Cursaru B, Stanescu P, Draghici C, Stanciu ND, Vuluga DM. Novel hydrogels from diepoxy-terminated poly(ethylene glycol)s and aliphatic primary diamines: synthesis and equilibrium swelling studies. Polym Advan Technol 2009;20:907-15.

[29] Zhou C, Truong VX, Qu Y, Lithgow T, Fu GD, Forsythe JS. Antibacterial poly(ethylene glycol) hydrogels from combined epoxy-amine and thiol-ene click reaction. J Polym Sci Pol Chem 2016;54:656-67.

[30] Mauri E, Veglianese P, Papa S, Mariani A, De Paola M, Rigamonti R, et al. Chemoselective functionalization of nanogels for microglia treatment. Eur Polym J 2017;94:143-51.

[31] Groot RD, Warren PB. Dissipative Particle Dynamics: Bridging the Gap between Atomistic and Mesoscopic Simulation. The Journal of Chemical Physics 1997;107:4423-35.

[32] Posel Z, Svoboda M, Lisal M. Controlled Transport of Flexible Polymers in Slit and Cylindrical Pores Coated with Polymer Brushes: Insight from Dissipative Particle Dynamics. J Nanosci Nanotechnol 2019;19:2943-9.

[33] van Krevelen DW, te Nijenhuis K. Properties of Polymers. Amsterdam: Elsevier; 2009.

[34] Khedr A, Striolo A. DPD Parameters Estimation for Simultaneously Simulating Water–Oil Interfaces and Aqueous Nonionic Surfactants. J Chem Theory Comput 2018;14:6460-71.

[35] Tang X, Zou W, Koenig PH, McConaughy SD, Weaver MR, Eike DM, et al. Multiscale Modeling of the Effects of Salt and Perfume Raw Materials on the Rheological Properties of Commercial Threadlike Micellar Solutions. J Phys Chem B 2017;121:2468-85.

[36] Ibergay C, Malfreyt P, Tidesley DJ. Electrostatic Interactions in Dissipative Particle Dynamics: Toward a Mesoscale Modeling of the Polyelectrolyte Brushes. J Chem Theory Comput 2009;5:3245-59.

[37] Warren PB, Vlasov A. Screening properties of four mesoscale smoothed charge models, with application to dissipative particle dynamics. J Chem Phys 2014;140:084904-9.

[38] Plimpton S. Fast Parallel Algorithms for Short-Range Molecular Dynamics. J Comp Phys 1995;117:1-19.

[39] Mauri E, Chincarini GMF, Rigamonti R, Magagnin L, Sacchetti A, Rossi F. Modulation of electrostatic interactions to improve controlled drug delivery from nanogels. Mat Sci Eng C-Mater 2017;72:308-15.

[40] Breunig M, Lungwitz U, Liebl R, Goepferich A. Breaking up the correlation between efficacy and toxicity for nonviral gene delivery. P Natl Acad Sci USA 2007;104:14454-9.

[41] Moghimi SM, Symonds P, Murray JC, Hunter AC, Debska G, Szewczyk A. A two-stage poly(ethylenimine)-mediated cytotoxicity: Implications for gene transfer/therapy. Mol Ther 2005;11:990-5.

[42] Sung SJ, Min SH, Cho KY, Lee S, Min YJ, Yeom YI, et al. Effect of polyethylene glycol on gene delivery of polyethylenimine. Biol Pharm Bull 2003;26:492-500.

[43] Shang L, Nienhaus K, Nienhaus GU. Engineered nanoparticles interacting with cells: size matters. J Nanobiotechnol 2014;12.

[44] Locatelli D, Terao M, Fratelli M, Zanetti A, Kurosaki M, Lupi M, et al. Human Axonal Survival of Motor Neuron (a-SMN) Protein Stimulates Axon Growth, Cell Motility, C-C Motif Ligand 2 (CCL2), and Insulin-like Growth Factor-1 (IGF1) Production. J Biol Chem 2012;287:25782-94.

[45] Mauri E, Cappella F, Masi M, Rossi F. PEGylation influences drug delivery from nanogels. J Drug Deliv Sci Tec 2018;46:87-92.

[46] Ziebarth JD, Wang YM. Understanding the Protonation Behavior of Linear Polyethylenimine in Solutions through Monte Carlo Simulations. Biomacromolecules 2010;11:29-38.

[47] Curtis KA, Miller D, Millard P, Basu S, Horkay F, Chandran PL. Unusual Salt and pH Induced Changes in Polyethylenimine Solutions. Plos One 2016;11.

[48] Jehser M, Zifferer G, Likos CN. Scaling and Interactions of Linear and Ring Polymer Brushes via DPD Simulations. Polymers 2019;11:541.

[49] Posel Z, Posocco P, Lisal M, Fermeglia M, Pricl S. Highly grafted polystyrene/polyvinylpyridine polymer gold nanoparticles in a good solvent: effects of chain length and composition. Soft Matter 2016;12:3600-11.

[50] Cheng L, Vishnyakov A, Neimark AV. Morphological Transformations in Polymer Brushes in Binary Mixtures: DPD Study. Langmuir 2014;30:12932-40.

[51] Chen L, Yan C, Zheng Z. Functional polymer surfaces for controlling cell behaviors Materials Today 2018;21:38-59.